

1

2 Antagonism of RNase L is required for murine coronavirus replication in Kupffer cells and liver
3 sinusoidal endothelial cells but not in hepatocytes

4 Yize Li and Susan R. Weiss

5 Department of Microbiology, Perelman School of Medicine, University of Pennsylvania, Philadelphia,
6 PA 19104

7

8

9 Running title: KC and LSEC limit MHV NS2 mutant liver replication

10 Key words: Murine coronavirus, MHV, phosphodiesterase, hepatocytes, Kupffer cells, liver
11 sinusoidal endothelial cell, hepatitis

*Corresponding Author

Susan R. Weiss
Department of Microbiology
University of Pennsylvania
Perelman School of Medicine
203A Johnson Pavilion
36th Street and Hamilton Walk
Philadelphia, PA 19104-6076
PHONE: 215-898-8013
FAX: 215-573-4858
Email: weissr@upenn.edu

Abstract: 250 words

Text: 3544 words

12 **ABSTRACT**

13 Mouse hepatitis virus strain A59 infection of mice is a useful tool for studying virus-host interaction
14 during hepatitis development. The NS2^{H126R} mutant is attenuated in liver replication due to loss of
15 phosphodiesterase activity, which the wild-type virus uses to block the 2',5'-oligoadenylate
16 synthetase (OAS)-ribonuclease L (RNase L) antiviral pathway. The activation of RNase L by
17 NS2^{H126R} is cell-type dependent and correlates with high basal expression levels of OAS, as found in
18 myeloid cells. We tested the hypothesis that resident liver macrophages, Kupffer cells (KC), are the
19 most likely cell type to restrict NS2^{H126R} and prevent hepatitis. As found previously, A59 and NS2^{H126R}
20 replicate similarly in hepatocytes and neither activates RNase L, as assessed by an rRNA
21 degradation assay. In contrast, in KCs, A59 exhibited a 100-fold higher titer than NS2^{H126R} and
22 NS2^{H126R} induced rRNA degradation. Interestingly, in liver sinusoidal endothelial cells (LSEC), the
23 cells that form a barrier between blood and liver parenchymal cells, NS2^{H126R} activates RNase L,
24 which limits viral replication. Similar growth kinetics were observed for both viruses in KC and LSEC
25 from RNase L^{-/-} mice, demonstrating that both use RNase L to limit NS2^{H126R} replication. Depletion of
26 KC by gadolinium(III) chloride or LSEC by cyclophosphamide partially restores liver replication of
27 NS2^{H126R}, leading to hepatitis. Thus, during MHV infection, hepatitis, which damages the
28 parenchyma, is prevented by RNase L activity in both KC and LSEC but not in hepatocytes. This
29 may be explained by the undetectable levels of RNase L as well as OASs expressed in hepatocytes.

30

31

32

33

34

35

36

37

38 **IMPORTANCE**

39 Mouse hepatitis virus infection of mice provides a useful tool for studying virus-host interactions
40 during hepatitis development. The NS2^{H126R} mutant is attenuated in liver replication due to loss of
41 phosphodiesterase activity, with which the wild-type virus blocks the potent OAS-RNase L antiviral
42 pathway. RNase L activation by NS2^{H126R} is cell-type dependent and correlates with high basal
43 expression levels of OAS, as found in myeloid cells. We showed that hepatocytes that comprise the
44 liver parenchyma do not activate RNase L when infected with NS2^{H126R} nor do they restrict
45 replication. However, both Kupffer cells (KC), liver resident macrophages and liver sinusoidal
46 endothelial cells (LSEC) which line the sinusoids activate RNase L in response to NS2^{H126R}. These
47 data suggest that KC and LSEC prevent viral spread into the parenchyma, preventing hepatitis.
48 Furthermore, hepatocytes express undetectable levels of OASs and RNase L, which likely explains
49 the lack of RNase L activation during NS2^{H126R} infection.

50

51

52

53

54

55

56

57

58

59

60

61

62

63

64 **INTRODUCTION**

65 Mouse hepatitis virus (MHV) belongs to the order *Nidovirales*, family *coronaviridae*, and genus
66 *Betacoronavirus*. Coronaviruses are enveloped, nonsegmented positive-strand RNA viruses (1).
67 MHV strain A59 induces moderate to severe hepatitis in infection of mice (2); replication and the
68 consequent liver pathogenesis are dependent on the 2',5'-phosphodiesterase (PDE) activity of the
69 viral accessory protein NS2 (3).

70 The 2',5'-oligoadenylate (2-5A) synthetase (OAS)-ribonuclease (RNase) L pathway is a potent IFN-
71 induced antiviral activity (4). Upon infection by diverse viruses, including the human liver pathogenic
72 hepatitis C virus (5, 6), dsRNA is detected by OAS proteins. Four mouse OAS species (OAS1a/g,
73 OAS2, OAS3 and OASL2) and 3 human OAS species (OAS1, OAS2, OAS3) can bind dsRNA *in*
74 *vitro* and be activated to generate 2-5A (7), the latter binding to and promoting activation and
75 dimerization of RNase L, which results in both cellular and viral RNA degradation and thus inhibition
76 of viral replication (7, 8).

77 The PDE (NS2) of MHV cleaves 2-5A and inhibits the activation of RNase L(3). An A59 mutant,
78 NS2^{H126R}, which encodes a catalytically inactive PDE replicates to a minimal extent in the mouse
79 liver and causes minor to no liver damage during infection (3). Previous studies have illuminated that
80 the activation of the OAS-RNase L antiviral pathway is cell type dependent. Bone marrow derived
81 macrophages (BMM) and bone marrow derived dendritic cells (BMDC) as well as microglia, brain
82 resident macrophages, limit NS2^{H126R} replication by activating the OAS-RNase L pathway. The basal
83 mRNA expression levels of OASs vary among the cell types and high levels of OAS correlate with
84 activation of the pathway (9, 10).

85 While the liver is known as a digestive organ, it also serves as an immunological organ (11-13). The
86 liver is composed of two populations of cells, including approximately 80% liver parenchymal cells
87 (hepatocytes) and 20% nonparenchymal cells (NPC). About 10% NPC are Kupffer cells (KC), or

88 liver macrophages, and 50% of NPC are liver sinusoidal endothelial cells (LSEC) (13). We found
89 previously that NS2^{H126R} infection failed to induce RNase L activation in hepatocytes and that
90 NS2^{H126R} replicated to similar extent as A59 in that cell type (9). However, little is known about the
91 activation of the OAS-RNase L pathway in the other liver cell types and specifically in which cell type
92 RNase L activation will limit NS2^{H126R} replication, although previous studies implicated a protective
93 role of KC(3). Here, we isolated the various primary liver cells and infected them with WT A59 and
94 NS2^{H126R} to assess the activation of RNase L as well as quantify viral replication from these cells.
95 We found KC and LSEC but not hepatocytes can limit NS2^{H126R} replication, indicating they have an
96 active OAS-RNase L pathway and this is likely due to differential levels of expression of RNase L as
97 well as OAS among these liver cell types. To further study the protective role of KC and LSEC, we
98 performed *in vivo* cell depletion in mice and showed depletion of KC or LSEC enhance NS2^{H126R} liver
99 replication and pathogenicity.

100 MATERIAL AND METHODS

101 **Cells lines, mice and viruses.** Mouse L2 fibroblasts were cultured as described previously (14).
102 Recombinant coronaviruses inf-MHV-A59 (A59) and inf-NS2^{H126R} (NS2^{H126R}) have been described
103 previously (15, 16). C57BL/6 (B6) mice were purchased from the National Cancer Institute
104 (Frederick, MD), and bred in the University of Pennsylvania animal facility. All procedures were
105 approved by the University of Pennsylvania Institutional Animal Care and Use Committee (IACUC).

106 **Isolation of primary liver cells.** Mice were euthanized with CO₂, and the livers were perfused.
107 Briefly, the animal was opened to expose the inferior vena cava (IVC) and portal vein, a catheter
108 was inserted into the IVC, and connected to a pump filled with dissociation buffer (NaCl, 8g/L, KCl,
109 0.4g/L, NaH₂PO₄ •H₂O, 78mg/L, Na₂HPO₄ 120.45mg/ml, HEPES, 2380mg/L, Na₂CO₃, 350mg/L,
110 ethylene glycol tetraacetic acid (EGTA), 190mg/L, glucose 900mg/L, pH=7.4). The portal vein was

111 cut immediately to allow the buffer (20-30 ml) to flow through the liver.

112 For hepatocytes, the liver was digested with collagenase IV (0.05%) (Sigma-Aldrich) in liver
113 digestion buffer (NaCl, 8g/L, KCl, 0.4g/L, NaH₂PO₄ •H₂O, 78mg/L, Na₂HPO₄ 120.45mg/ml, HEPES,
114 2380mg/L, Na₂CO₃, 350mg/L, phenol red, 6mg/L, CaCl₂ •2H₂O, 560mg/L, pH=7.4). After digestion,
115 the liver was removed from the mouse and cells were dissociated from Glisson's capsule and were
116 filtered through a 100µm cell strainer (Becton Dickinson, BD). The cells were centrifuged at 40×g for
117 3min at 4°C, and the pellet was re-suspended in digestion buffer containing 1mg/ml DNase I
118 (Roche). The cells were centrifuged and washed with MEM (minimum essential medium Eagle,
119 Sigma-Aldrich) three times and were re-suspended in William's E media (Gibco) supplemented with
120 10% FBS, 100U/ml of penicillin and 100mg/ml streptomycin, 2mM L-Glutamine. The cells were
121 placed on plates coated with rat-tail collagen (Sigma-Aldrich). Four hours after plating, the cells were
122 washed with phosphate buffer saline (PBS) and used for experimentation.

123 Kupffer cells (KC) were isolated from mixed primary liver cell cultures using previously described
124 methods (17). Briefly, after perfusion with dissociation buffer, the liver was digested with collagenase
125 I (0.05%)(Sigma-Aldrich) in digestion buffer supplemented with 50µg/ml Trypsin inhibitor (Sigma-
126 Aldrich). Cells were harvested and washed three times with MEM, and cultured in DMEM (Gibco,
127 10566) supplemented with 10% FBS, 100U/ml of penicillin and 100mg/ml streptomycin, 100µM β-
128 mercaptoethanol, 10µg/ml insulin, 10mM HEPES and 50µg/ml gentamicin, in a flask coated with rat-
129 tail collagen, 1X10⁷ cells per T175 flask. The next day, the flasks were shaken to remove the dead
130 cells, and on days 4 and day 7, fresh medium was added and the KC were harvested at days 9 to 12
131 post plating by shaking and then selected by binding to a petri dish (BD). KC were recovered by
132 TrpLE select enzyme (Invitrogen) digestion and plated for experiments.

133 The liver sinusoidal endothelial cell (LSEC) isolation protocol was adapted from previously described

134 methods (18). Briefly, after perfusion with dissociation buffer, the liver was digested with collagenase
135 I (0.025%) and collagenase II (0.025%)(Sigma-Aldrich) in digestion buffer supplemented with
136 50µg/ml Trypsin inhibitor (Sigma-Aldrich). After digestion, the liver was removed and cells were
137 dissociated from Glisson's capsule in preservation buffer [NaCl, 4.15g/L, 0.25g/L KCl, 1.12g/L
138 HEPES, 0.24g/L NaOH, bovine serum albumin (BSA),10g/L)], and filtered through a 100µm cell
139 strainer (BD). The supernatant was centrifuged at 60×g for 2 min three times to remove
140 parenchymal cells. The supernatant was further centrifuged at 1350×g 4°C for 10min to harvest the
141 non-parenchymal cells (NPC). The NPC were re-suspended in preservation buffer and were applied
142 on top of a 25/50% Percoll (GE Amersham) bilayer. The cells were centrifuged at 1350×g 4°C for
143 10min. LSEC and KC were collected from the interface between the two density layers.. Cells were
144 washed with preservation buffer and resuspended in RPMI 1640 medium (Gibco) supplemented
145 with100U/ml of penicillin and 100mg/ml streptomycin. Cells then were plated onto a petri dish and
146 incubated for 8 min to remove KC which attach to the surface; the removal of KC was repeated once
147 more. The supernatant containing the LSEC was harvested and centrifuged at 1350×g 4°C for
148 10min. The pellet was resuspended in RPMI 1640 medium (Gibco) supplemented with 100U/ml of
149 penicillin and 100mg/ml streptomycin and placed onto rat-tail collagen coated plates. Two hours
150 after plating, the cells were washed vigorously with ice cold PBS twice. The cells remaining on the
151 plates were used for further experiments.

152 **Antibodies.** Mouse anti human HNF-4α (cross reactive with mouse HNF-4α) monoclonal antibody
153 (mAb) (5µg/ml, R&D), and goat anti mouse IgG conjugated to Alexa Fluor-488 (1:400, Invitrogen)
154 were used to detect HNF-4α by immunofluorescence assay (IFA); rat anti mouse CD68 (1:100,
155 Serotech) mAb, conjugated to Alexa Fluor-488 were used to detect CD68 by IFA. OAS1A (clone E-
156 2, Santa Cruz; 1:200) mAb, OAS2 (clone G-9, Santa Cruz, 1:200), OAS3 (clone D-7, Santa Cruz,
157 1:200), goat anti RNase L (clone T-16, Santa Cruz, 1:200), as well as anti-GAPDH (Thermo-Fisher,
158 1:1000), goat anti-mouse IgG-HRP (Santa Cruz, 1:5000), and donkey anti-goat IgG-HRP (1:5000)

159 secondary antibodies were used to detect the primary antibodies of the appropriate species.

160 **Immunolabeling.** Cells were fixed in PBS containing 4% paraformaldehyde (Bio-Rad), blocked with
161 2% BSA, and immunolabeling with anti HNF-4 α antibodies was used to detect hepatocytes;
162 immunolabeling with anti-CD68 antibodies conjugated with Alexa Fluor-488 was used to distinguish
163 KC (CD68 positive) and LSEC (CD68 negative). Primary anti-HNF-4 α antibody was detected with
164 goat anti-mouse Alexa Fluor 488 (Invitrogen). DAPI (4',6-Diamidino-2-Phenylindole, Dihydrochloride)
165 (Invitrogen) was used to stain the nucleus. Fluorescence was visualized with a Nikon Eclipse 2000E-
166 U fluorescence microscope, and images were acquired using Nikon NIS-Element BR software
167 (Nikon)

168 Low density lipoprotein (LDL) uptake assay of LSEC. After isolation, cells were cultured in RPMI
169 1640 without FBS, medium containing 5 μ g/ml of LDL conjugated with Alexa Fluor-488 (Invitrogen)
170 was added, the cells were incubated at 37°C for 4 hours, and at 30 minutes before imaging, 1 μ g/ml
171 of Hoechst (Sigma-Aldrich) was add to the medium. Fluorescence was visualized with a Nikon
172 Eclipse 2000E-Ufluorescence microscope, and images were acquired using Nikon NIS-Element BR
173 software(Nikon)

174 **Virus growth kinetics.** Hepatocytes (1.5X10⁵ cell per well in 24-well plates), KC (1X10⁵ cell in 48-
175 well plates) or LSEC (5.0X10⁵ cell per well in 48-well plates) were infected with A59 or NS2^{H126R}
176 (MOI=1 PFU/cell) and at the indicated time points, cells and supernatants were harvested together,
177 and then frozen (-80°C) and thawed three times and finally viruses were titrated by L2 cell plaque
178 assay (19).

179 **KC and LSEC depletion and MHV infection.** Gadolinium(III) chloride was used deplete KC from
180 the livers of mice. B6 mice were intravenously injected with 20mg/kg of Gadolinium(III) chloride in
181 100 μ l of saline (20). Cyclophosphamide was used to deplete LSEC from the livers of mice. B6 mice

182 were intraperitoneally (i.p.) injected with 300mg/kg of cyclophosphamide in 200 μ l saline. Twenty-four
183 hours post injection, mice were infected with 200 pfu of virus intrahepatically (i.h.). On day 5 post
184 infection, mice were sacrificed and livers were harvested for virus titration (19) and histological
185 analysis (3).

186 **Western blotting.** Cells were treated or mock treated with 1000U of IFN- α (PBL) overnight,
187 harvested and washed in PBS and lysed with NP40 buffer [1% NP-40, 2 mM EDTA, 10% glycerol
188 150 mM NaCl, 50 mM Tris pH 8.0) with protease inhibitor cocktail (Roche)]. Cell lysates were mixed
189 with 4X Laemmli buffer and boiled at 95°C for 5 minutes and analyzed by electrophoresis on 4-15%
190 gradient SDS gels. Proteins were transferred to polyvinylidene difluoride (PVDF) membranes, which
191 were treated with 5% nonfat milk in TBST (Tris-HCl buffer saline with 0.5% Tween-20) blocking
192 buffer for one hour, followed by incubation overnight at 4°C with antibodies diluted into TBST.
193 Membranes were then washed three times with TBST and incubated with secondary antibodies for 1
194 hour at room temperature, washed three times with TBST and then incubated with SuperSignal
195 West Dura Extended Duration substrate (Thermo) and the signal was detected using an Amersham
196 Imager 600 (GE).

197
198 **Histology.** Livers were isolated and fixed in 4% paraformaldehyde, embedded in paraffin and
199 sectioned. Sections were stained with hematoxylin and eosin as described previously (3).

200

201 **Statistical analysis.** Two-tailed student t-test was performed to determine statistically significant
202 differences for *in vitro* experiments. The Mann-Whitney test was used to analyze differences in virus
203 titer in different mouse tissues. Any undetectable titers from *in vitro* and *in vivo* infections were
204 entered as the limit of detection value for each experiment. All data were analyzed by using Prism
205 software (GraphPad Software, Inc., CA).

206 **RESULTS**

207 **Isolation and purification of Kupffer cells (KC), liver sinusoidal endothelial cells (LSEC) and**
208 **hepatocytes from mouse liver**

209 To study the role of individual liver cell types in limiting NS2^{H126R} replication, we purified each of the
210 three major cell types, representing >95% of liver cells, and cultured them *in vitro*. Specifically, we
211 focused on the parenchymal cells (the hepatocytes) and the non-parenchymal Kupffer cells (KC)
212 and liver sinusoidal endothelial cells (LSEC), using established isolation and culture methods, as
213 described elsewhere (17, 18). To assess the purity of the liver cell preparations, we used the
214 nonspecific stain DAPI in all the tests to identify the nuclei. To identify hepatocytes, we stained with
215 an antibody that recognizes hepatocyte nuclear factor 4 α (HNF4 α), a marker for hepatocytes (green)
216 (21). Over 99% of the cells in the hepatocyte preparation were HNF-4 α positive, as seen in Fig 1A-
217 C, which show the merged blue and green stains. KC cells, the resident liver macrophages, were
218 detected by immunostaining for CD68 (Fig 1D), a KC specific marker (22). In the KC-purified
219 preparation, we found that >95% the cells were CD68-positive cells. LSEC were isolated from total
220 liver non-parenchymal cells. LSEC readily take up LDL (low density lipoprotein) (23). Therefore, we
221 incubated the LSEC with Alexa Fluor-488-conjugated-LDL for 2 hours, and then monitored the cells.
222 Over 95% of the cells were Alexa Fluor-488 positive (Fig 1F). To confirm there was little to no KC
223 cell contamination, the LSEC were stained with anti-CD68 antibodies; less than 1% of cells were
224 CD68 positive cells (Fig 1E). These results indicate that our isolation methods for hepatocytes, KC
225 and LSEC yielded highly purified products.

226

227 **Kupffer cells (KC) and liver sinusoidal endothelial cells (LSEC) but not hepatocytes limit**
228 **NS2^{H126R} replication *in vitro* through activation of RNase L.** To determine which cells limit
229 NS2^{H126R} replication, hepatocyte, KC, and LSEC cells derived from B6 (WT) and RNase L KO mice
230 were infected *in vitro* with WT A59 and mutant NS2^{H126R}. As observed previously in B6 hepatocytes,
231 A59 and NS2^{H126R} replicated similarly (9). However, in B6 KC and LSEC, A59 showed 10-100 fold

232 higher titer than NS2^{H126R} at 15 and 24 hours post-infection. When KC and LSEC from RNase L KO
233 mice were infected with NS2^{H126R}, the virus replicated to a similar titer as A59. These results suggest
234 that both KC and LSEC limit NS2^{H126R} virus replication by activation of the OAS-RNase L pathway,
235 as evidenced by the fact that replication in both these cell types was robust in cells from RNase L
236 KO mice and minimal in cells from B6 animals. To directly determine whether RNase L is activated
237 in KC and LSEC, cultures of each liver cell type as well as BMM, were infected with A59 and
238 NS2^{H126R} and at 12 hour (KC and BMM), 13 hour (LSEC), 15 hour (hepatocytes) post infection cells
239 were lysed total cellular RNA was harvested and analyzed for degradation by a Bioanalyzer, as
240 shown in Fig 3. Degradation of ribosomal RNA (rRNA) was observed in KC, LSEC and BMM but not
241 hepatocytes, consistent with the replication phenotype (Fig 2).

242

243 **Depletion of either KC or LSEC from mouse liver partially restores NS2^{H126R} replication and**
244 **liver pathogenicity.** To determine the role of KC and LSEC during MHV infection of intact animals,
245 KC or LSEC were depleted from the livers of B6 mice by intravenous injection of Gadolinium(III)
246 chloride (KC depletion) (20) or by intraperitoneal injection of cyclophosphamide (LSEC
247 depletion)(20, 24). The depletion of KC was monitored by India ink uptake which occurs only by KC
248 (25) and the disruption of the endothelial barrier was monitored by morphology as assessed by
249 electronic microscopy (24). We observed that >80% of KC or >50% of LSEC cells were depleted
250 from mouse liver (data not shown). Following depletion of KC from B6 mice, NS2^{H126R} replicated to
251 100-500 fold higher level than in the non-depleted livers. The depletion of LSEC showed a less
252 dramatic increase in virus titer than KC depletion but titers were still significantly higher than that in
253 the control mice (Fig 4A). Liver pathogenicity was monitored by H&E staining of liver sections (Fig
254 4B). Necrosis was readily apparent in livers from KC- and LSEC-depleted samples, but not in the
255 non-depleted animals. These results suggest that both the KC and LSEC protect the liver from
256 coronavirus infection *in vivo*.

257

258 **Hepatocytes express undetectable levels of RNase L and OAS.** Previous studies have indicated
259 that the activation of the OAS-RNase L pathway by NS2^{H126R} is cell type dependent and independent
260 of virus-induced IFN (3, 9). High basal levels of OAS mRNA and protein expression correlate with
261 activation of RNase L while RNase L expression was similar across the cell types examined,
262 including several primary CNS derived primary cells as well as BMM and BMDC (10) . Since we
263 found that among liver cells, the OAS-RNase L pathway can be activated in KC and LSEC but not in
264 hepatocytes, we hypothesized that KC and LSEC might have higher basal expression levels of OAS
265 genes than hepatocytes. Thus we assessed the basal and IFN induced expression levels of OAS1a,
266 OAS2, OAS3 and RNase L protein in hepatocytes, KC and LSEC by western blotting. OAS1a was
267 detected in KC and LSEC with or without IFN treatment (Fig 5) but not in hepatocytes. OAS2 was
268 not detected in any cell type without IFN treatment; however, OAS2 was induced to a detectable
269 level by IFN in KC. Basal expression of OAS3 was detected in KC but not in hepatocytes and LSEC;
270 however upon IFN treatment, OAS3 was further induced in KC and detected in LSEC but not
271 hepatocytes. The results are consistent with our previous data, in that myeloid cells express higher
272 basal levels of OAS genes and that murine OAS mRNA is induced by IFN treatment (9, 10, 26).
273 RNase L is constitutively expressed in many types of cells and is not generally induced by IFN
274 treatment (9, 10, 26). Surprisingly, while we detected RNase L in KC and LSEC, RNase L
275 expression was below the level of detection in hepatocytes. Consistent with the immunoblot data,
276 RNase L mRNA as quantified by qRT-PCR was also 100-1000 fold lower in hepatocytes as
277 compared with KC and LSEC (data not shown), suggesting there is very tight control of this pathway
278 in this cell type.

279

280 **DISCUSSION**

281 Based on previous findings that the OAS-RNase L pathway can be activated in BMM and BMDC as
282 well as microglia during NS2^{H126R} infection (9, 10), it is not surprising that the KC also activate
283 RNase L in response to viral infection. KC can be divided into two populations, one is yolk sac
284 derived which develop in the liver before the formation of bone marrow and the other population is
285 myeloid derived (27). A previous study showed that the yolk sac derived KC play roles in
286 immunosuppression, while myeloid derived KC are more immune active(27). We would predict that
287 the myeloid derived cells will be more readily activated to degrade RNA during viral infection and
288 future studies will include separating these types of KC and determining whether the two populations
289 have differences in the activation of the OAS-RNase L pathway during infection.

290

291 LSEC and KC form a barrier between the parenchymal hepatocytes and the blood (12, 13). Previous
292 studies showed that depletion of KC from rat or mouse liver improves the efficacy of gene therapy
293 mediated by lentivirus and adenovirus vectors (25). We have shown here that depletion of KC or
294 LSEC leads to a partial restoration of NS2^{H126R} liver replication, demonstrating that KC and LSEC
295 protect the liver from infection by limiting viral replication through activation of OAS-RNase L antiviral
296 pathways. These data are consistent with a previous reported that IFN signaling in myeloid cells was
297 crucial for protection from MHV induced hepatitis (28) and extend this finding to show that RNase L
298 activity specifically can restrict MHV NS2 mutant replication in the liver. Indeed, this is the first report
299 to find that KC and LSEC use the OAS-RNase L pathway to protect the mouse from viral liver
300 infection. It will be important to determine if this pathway limits other viral infections of the liver.

301

302 A key characteristic of LSEC is fenestration; these cells forms pores with diameters of 100-200nm
303 (29). While viruses need to cross the fenestration to infect hepatocytes, our results suggest that
304 MHV either cannot cross the fenestration or can cross inefficiently. Our results suggests that LSEC
305 limit MHV NS2^{H126R} liver spread by activation of the OAS-RNase L antiviral pathway as well as by
306 formation of a physical barrier. We previously observed in the primary cells derived from the central

307 nervous system that while activation of the OAS-RNase L pathway occurs in microglia, cells of
308 myeloid lineage, non-myeloid cells such as neurons or astrocytes could not be activated (9). LSECs
309 are the first example of non-myeloid cells in which rRNA degradation and inhibition of viral
310 replication are observed in NS2^{H126R} infection. This may reflect their role in protecting the liver
311 parenchyma from viral invasion.

312

313 RNase L is constitutively expressed in many types of cells, including myeloid and non-myeloid and is
314 not induced by IFN treatment (10, 26). While OAS genes are induced by IFN, the activation of the
315 OAS-RNase L pathway in myeloid cells is not dependent on induction of IFN during viral infection
316 (10, 26). Rather, it is the high basal expression level of OAS proteins that play a key role in
317 activation of the pathway (10). We found that by reducing the levels of basal OAS gene expression
318 in BMM we were able to prevent RNase L activation (10). Thus we hypothesized that lack of RNase
319 L activation in hepatocytes would be due to low basal expression levels of OAS genes. We were
320 surprised to find undetectable levels of RNase L as well as OAS1a, OAS2 and OAS3 in
321 hepatocytes, which would provide an explanation for the lack of RNA degradation observed in virus-
322 infected cells. This was the first cell type in which we found a lack of activation of the OAS-RNase
323 pathway correlated with low expression of RNase L as well as low levels of basal expression of
324 OAS. We speculate that since the liver has many pathogens and debris flowing through the
325 sinusoids, this may induce type I IFN expression and subsequently activation of RNase L, which can
326 lead to apoptosis (30). Thus, parenchymal hepatocytes have tightly controlled the OAS-RNase L
327 pathway, which may protect them from pathogen induced cell death, which can result from RNase L
328 activation.

329

330

331 **ACKNOWLEDGEMENTS**

332 This work was supported by NIH grants R01-AI104887 and R01-NS081008 to SRW. We thank Dr.
333 Ekihiro Seki, Dr. Maryna Perepelyuk, and Dr. Rebecca Wells for advice on isolating and culturing
334 primary liver cells, and Dr. Yan Wang for help with the intravenous catheterization.

335

336

337

338

339

340

341

342

343

344

345

346

347

348

349

350

351

352

353

354

355

356

357 **REFERENCES**

- 358 1. **Cavanagh D.** 1997. Nidovirales: a new order comprising Coronaviridae and Arteriviridae.
359 Arch Virol **142**:629-633.
- 360 2. **Weiss SR, Leibowitz JL.** 2011. Coronavirus pathogenesis. Adv Virus Res **81**:85-164.
- 361 3. **Zhao L, Jha BK, Wu A, Elliott R, Ziebuhr J, Gorbalenya AE, Silverman RH, Weiss SR.**
362 2012. Antagonism of the interferon-induced OAS-RNase L pathway by murine coronavirus
363 ns2 protein is required for virus replication and liver pathology. Cell Host Microbe **11**:607-
364 616.
- 365 4. **Dong B, Silverman RH.** 1995. 2-5A-dependent RNase molecules dimerize during activation
366 by 2-5A. J Biol Chem **270**:4133-4137.
- 367 5. **Han JQ, Barton DJ.** 2002. Activation and evasion of the antiviral 2'-5' oligoadenylate
368 synthetase/ribonuclease L pathway by hepatitis C virus mRNA. Rna-a Publication of the Rna
369 Society **8**:512-525.
- 370 6. **Washenberger CL, Han JQ, Kechris KJ, Jha BK, Silverman RH, Barton DJ.** 2007.
371 Hepatitis C virus RNA: dinucleotide frequencies and cleavage by RNase L. Virus Res
372 **130**:85-95.
- 373 7. **Kakuta S, Shibata S, Iwakura Y.** 2002. Genomic structure of the mouse 2',5'-oligoadenylate
374 synthetase gene family. J Interferon Cytokine Res **22**:981-993.
- 375 8. **Justesen J, Hartmann R, Kjeldgaard NO.** 2000. Gene structure and function of the 2'-5'-
376 oligoadenylate synthetase family. Cell Mol Life Sci **57**:1593-1612.
- 377 9. **Zhao L, Birdwell LD, Wu A, Elliott R, Rose KM, Phillips JM, Li Y, Grinspan J, Silverman
378 RH, Weiss SR.** 2013. Cell-type-specific activation of the oligoadenylate synthetase-RNase L
379 pathway by a murine coronavirus. J Virol **87**:8408-8418.
- 380 10. **Birdwell LD, Zalinger ZB, Li Y, Wright PW, Elliott R, Rose KM, Silverman RH, Weiss SR.**
381 2016. Activation of RNase L by Murine Coronavirus in Myeloid Cells Is Dependent on Basal
382 Oas Gene Expression and Independent of Virus-Induced Interferon. J Virol **90**:3160-3172.
- 383 11. **Racanelli V, Rehermann B.** 2006. The liver as an immunological organ. Hepatology
384 **43**:S54-S62.
- 385 12. **Crispe IN.** 2009. The liver as a lymphoid organ. Annu Rev Immunol **27**:147-163.
- 386 13. **Racanelli V, Rehermann B.** 2006. The liver as an immunological organ. Hepatology
387 **43**:S54-62.
- 388 14. **Yount B, Denison MR, Weiss SR, Baric RS.** 2002. Systematic assembly of a full-length
389 infectious cDNA of mouse hepatitis virus strain A59. J Virol **76**:11065-11078.
- 390 15. **Roth-Cross JK, Stokes H, Chang G, Chua MM, Thiel V, Weiss SR, Gorbalenya AE,
391 Siddell SG.** 2009. Organ-specific attenuation of murine hepatitis virus strain A59 by
392 replacement of catalytic residues in the putative viral cyclic phosphodiesterase ns2. J Virol
393 **83**:3743-3753.
- 394 16. **Schwarz B, Routledge E, Siddell SG.** 1990. Murine coronavirus nonstructural protein ns2 is
395 not essential for virus replication in transformed cells. J Virol **64**:4784-4791.
- 396 17. **Kitani H, Takenouchi T, Sato M, Yoshioka M, Yamanaka N.** 2011. A Simple and Efficient
397 Method to Isolate Macrophages from Mixed Primary Cultures of Adult Liver. Jove-Journal of
398 Visualized Experiments.
- 399 18. **Oie CI, Appa RS, Hilden I, Petersen HH, Gruhler A, Smedsrod B, Hansen JB.** 2011. Rat
400 liver sinusoidal endothelial cells (LSECs) express functional low density lipoprotein receptor-
401 related protein-1 (LRP-1). J Hepatol **55**:1346-1352.
- 402 19. **Gombold JL, Hingley ST, Weiss SR.** 1993. Fusion-defective mutants of mouse hepatitis
403 virus A59 contain a mutation in the spike protein cleavage signal. J Virol **67**:4504-4512.
- 404 20. **Duffield JS, Forbes SJ, Constandinou CM, Clay S, Partolina M, Vuthoori S, Wu S, Lang
405 R, Iredale JP.** 2005. Selective depletion of macrophages reveals distinct, opposing roles
406 during liver injury and repair. J Clin Invest **115**:56-65.
- 407 21. **Li J, Ning G, Duncan SA.** 2000. Mammalian hepatocyte differentiation requires the
408 transcription factor HNF-4alpha. Genes Dev **14**:464-474.

- 409 22. **Klein I, Cornejo JC, Polakos NK, John B, Wuensch SA, Topham DJ, Pierce RH, Crispe**
410 **IN.** 2007. Kupffer cell heterogeneity: functional properties of bone marrow-derived and
411 sessile hepatic macrophages. *Blood* **110**:4077-4085.
- 412 23. **Ling W, Lougheed M, Suzuki H, Buchan A, Kodama T, Steinbrecher UP.** 1997. Oxidized
413 or acetylated low density lipoproteins are rapidly cleared by the liver in mice with disruption of
414 the scavenger receptor class A type I/II gene. *J Clin Invest* **100**:244-252.
- 415 24. **Malhi H, Annamaneni P, Slehria S, Joseph B, Bhargava KK, Palestro CJ, Novikoff PM,**
416 **Gupta S.** 2002. Cyclophosphamide disrupts hepatic sinusoidal endothelium and improves
417 transplanted cell engraftment in rat liver. *Hepatology* **36**:112-121.
- 418 25. **van Til NP, Markusic DM, van der Rijt R, Kunne C, Hiralall JK, Vreeling H, Frederiks**
419 **WM, Oude-Elferink RP, Seppen J.** 2005. Kupffer cells and not liver sinusoidal endothelial
420 cells prevent lentiviral transduction of hepatocytes. *Mol Ther* **11**:26-34.
- 421 26. **Li YZ, Banerjee S, Wang YY, Goldstein SA, Dong BH, Gaughan C, Silverman RH, Weiss**
422 **SR.** 2016. Activation of RNase L is dependent on OAS3 expression during infection with
423 diverse human viruses. *Proc Natl Acad Sci U S A* **113**:2241-2246.
- 424 27. **Schulz C, Gomez Perdiguero E, Chorro L, Szabo-Rogers H, Cagnard N, Kierdorf K,**
425 **Prinz M, Wu B, Jacobsen SE, Pollard JW, Frampton J, Liu KJ, Geissmann F.** 2012. A
426 lineage of myeloid cells independent of Myb and hematopoietic stem cells. *Science* **336**:86-
427 90.
- 428 28. **Cervantes-Barragan L, Kalinke U, Züst R, König M, Reizis B, Lopez-Macias C, Thiel V,**
429 **Ludewig B.** 2009. Type I IFN-mediated protection of macrophages and dendritic cells
430 secures control of murine coronavirus infection. *J Immunol* **182**:1099-1106.
- 431 29. **Elvevold K, Smedsrod B, Martinez I.** 2008. The liver sinusoidal endothelial cell: a cell type
432 of controversial and confusing identity. *Am J Physiol Gastrointest Liver Physiol* **294**:G391-
433 400.
- 434 30. **Castelli JC, Hassel BA, Maran A, Paranjape J, Hewitt JA, Li XL, Hsu YT, Silverman RH,**
435 **Youle RJ.** 1998. The role of 2'-5' oligoadenylate-activated ribonuclease L in apoptosis. *Cell*
436 *Death Differ* **5**:313-320.
- 437

438

439

440

441

442

443

444

445

446

447

448

449 **FIGURE LEGENDS**

450

451 Figure 1. Isolation and characterization of hepatocytes (Hep), KC and LSEC. Hep, KC and LSEC
452 were isolated as described in Materials and Methods, (A) Hep were stained with mouse anti human
453 HNF-4 α and followed by secondary Alexa488-conjugated goat anti mouse antibody (Green), (B)
454 DAPI and (C) both stains merged. (D) KC and (E) LSEC were stained with Alexa Fluor -488
455 conjugated anti-CD68 antibodies (Green) and with DAPI to identify the nuclei. (F) LSEC were
456 incubated with Alexa Fluor-488 conjugated LDL (Green) in serum free media at 5 μ g/ml for 2 hours
457 and Hoechst (Blue) was added in the media the to stain the nucleus 30 minutes before imaging.

458

459 Figure 2. The replication of NS2^{H126R} is limited in KC and LSEC isolated from B6 mice but not from
460 RNase L^{-/-} mice. (A) Hepatocytes (Hep) from B6 mice, (B) KC from B6 mice (C) KC from RNase L^{-/-}
461 mice; (D) LSEC from B6 mice, (E) LSEC from RNase L^{-/-} mice were infected with A59 and NS2^{H126R}
462 (MOI=1, n=3). At the indicated time points, infectious virus was quantified by plaque assay on L2
463 cells from the combined cell lysates and supernatants. Data shown were analyzed by two-tailed
464 student t-test and expressed as means \pm S.D. (***, $P < 0.001$) and are from one representative of two
465 independent experiments.

466

467

468 Figure 3. RNase L is activated in BMM, KKC and LSEC but not hepatocytes (Hep) during infection
469 with NS2^{H126R}. BMM, hepatocytes, KC and LSEC were infected with MHV A59 and ns2^{H126R} (MOI=1).
470 At twelve hours (BMM and KC), 13 hours (LSEC) or 15 hours (Hep) post infection, RNA was
471 harvested and analyzed by a Bioanalyzer, for ribosomal RNA (rRNA) integrity. The positions of 28S
472 and 18S rRNA are indicated. Data shown are from one representative of two independent
473 experiments.

474

475 Figure 4. Depletion of KC or LSEC partially restores NS2^{H126R} replication and liver pathogenicity. B6
476 mice were intravenously injected with 20mg/kg of gadolinium(III) chloride (KC depletion) or
477 intraperitoneally injected with 300mg/kg of cyclophosphamide (LSEC depletion) or with saline as
478 control (n=5 for each group). Twenty-four hours post injection, mice were infected with 200 pfu of
479 virus intrahepatically and sacrificed 5 days pi. (A) Virus was quantified from liver lysates by plaque
480 assay on L2 cells. The data were analyzed by the Mann-Whitney test and expressed as mean \pm SD
481 (**, p<0.01; ***, p< 0.001, titers in depleted mice compared to the saline control). B. Liver sections
482 from NS2^{H126R} infected mice were stained with hematoxylin and eosin for histological analysis.
483 Arrows indicate foci of pathology. Data shown as are from one representative of two independent
484 experiments.

485

486 Figure 5. Expression of OAS1a, OAS2, OAS3 and RNase L are below the level of detection in
487 hepatocytes. Hepatocytes (Hep), KC and LSEC were mock treated or treated with IFN- α (1000U/ml)
488 overnight. Cells were lysed, and proteins were analyzed by immunoblotting with antibodies against
489 OAS1a, OAS2, OAS3, RNase L and GAPDH. The positions and molecular weights of the indicated
490 proteins are indicated with arrows. Data shown as are from one representative of two independent
491 experiments. The additional bands detected with OAS2 antibody in all cell types and with OAS3
492 antibody in Hep and LSEC are not induced by IFN as expected for OAS proteins and are nonspecific
493 (10).

494

495

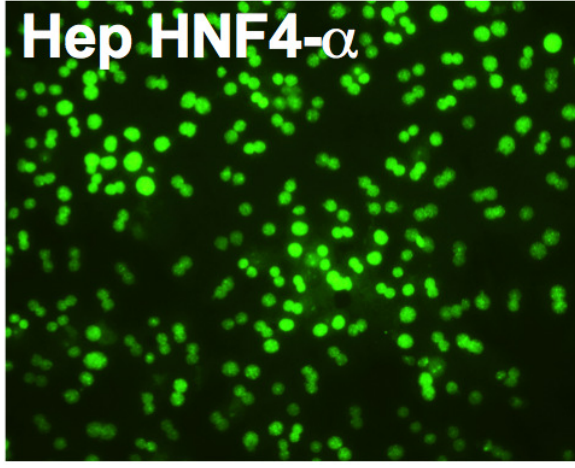
496

497

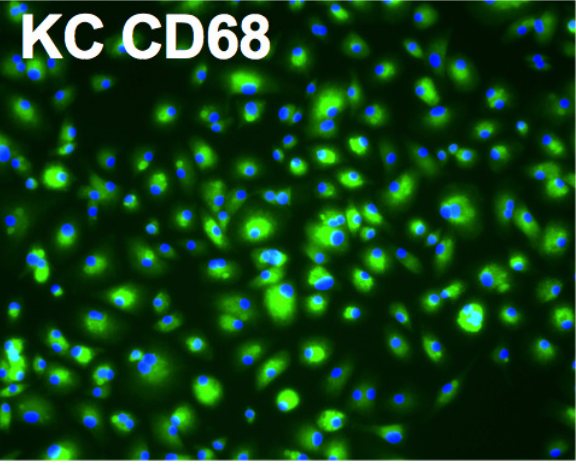
498

499

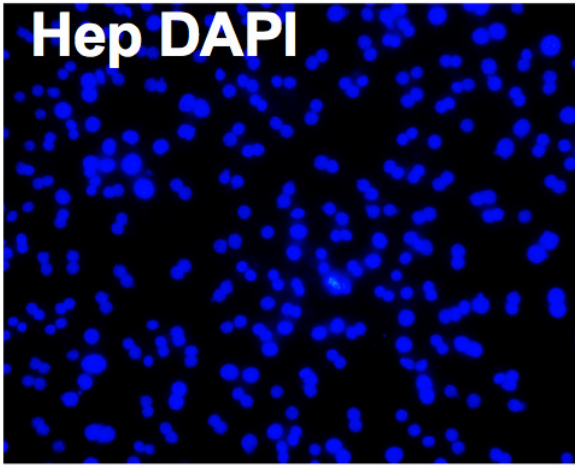
A



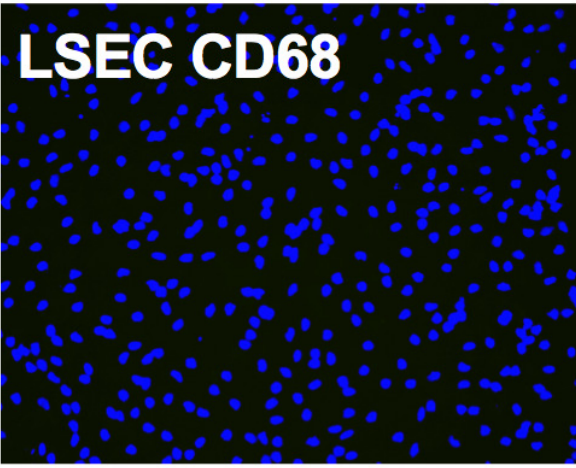
D



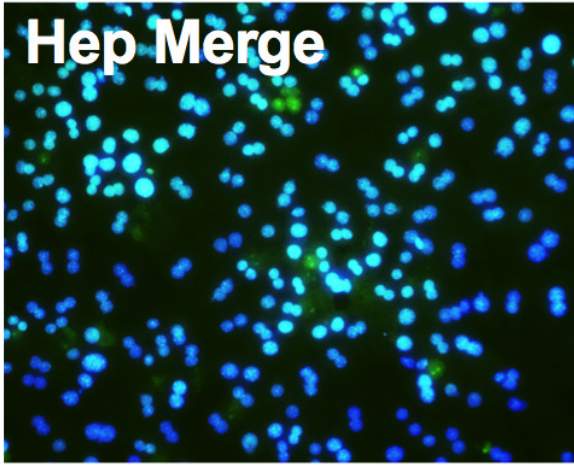
B



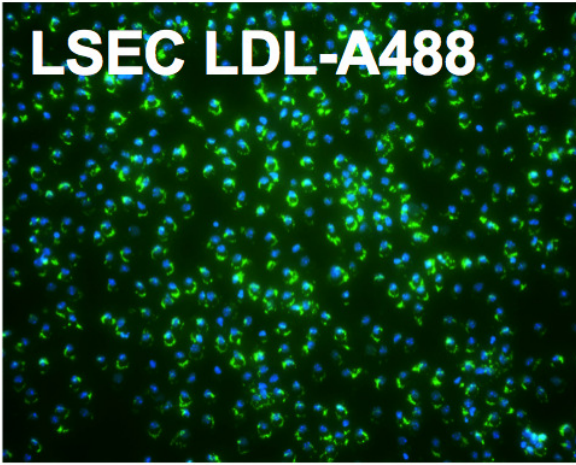
E

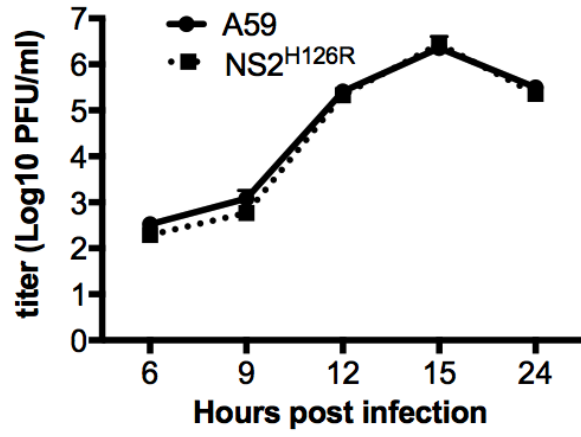
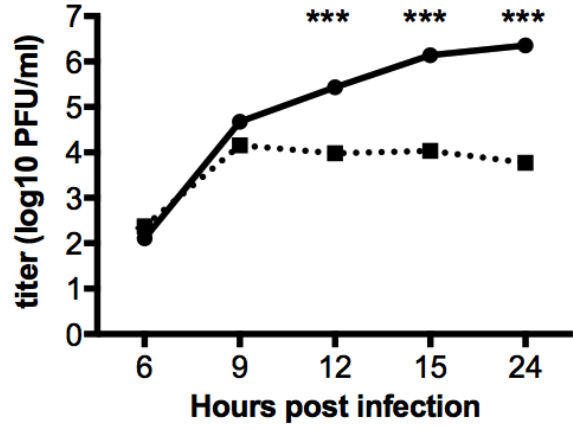
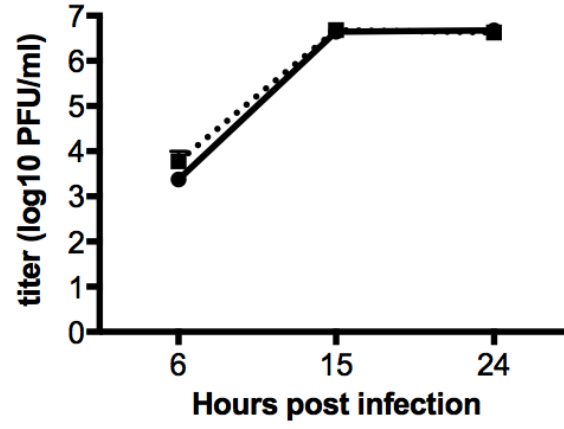
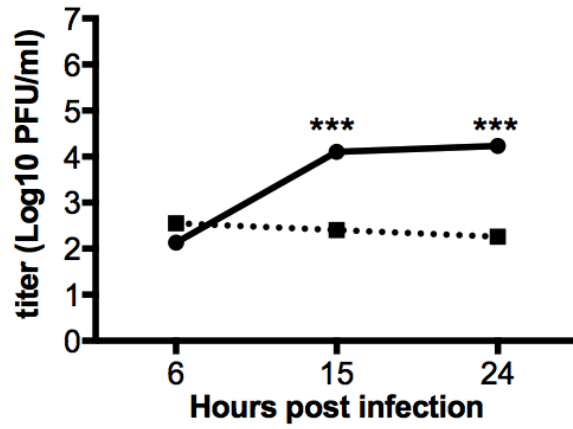


C



F



A**B****C****D****E**